Available online at www.sciencedirect.com

SCIENCE DIRECT®

Tectonophysics 421 (2006) 299–317

TECTONOPHYSICS

www.elsevier.com/locate/tecto

The thermal evolution of Corsica as recorded by zircon fission-tracks

M. Giuditta Fellin [a,b,*], Joseph A. Vance [c], John I. Garver [d], Massimiliano Zattin [a]

[a] *Dipartimento di Scienze della Terra e Geologico-Ambientali, Alma Mater Studiorum — Università di Bologna, Via Zamboni 67, 40126 Bologna, Italy*

[b] *Dipartimento di Geologia, Paleontologia e Geofisica, Università di Padova, Via Giotto 1, 35122 Padova, Italy*

[c] *Department of Earth and Space Sciences, University of Washington, Seattle, Washington, 98195, USA*

[d] *Geology Department, Union College, Schenectady, New York, 12308, USA*

Received 28 November 2005; received in revised form 27 April 2006; accepted 4 May 2006
Available online 21 June 2006

Abstract

New zircon fission-track (ZFT) ages from Corsica record multiple thermal events that can be tied to the structural evolution of the western Mediterranean region. The Corsican zircons have a wide scatter of ZFT grain ages (243–14 Ma), which together define several age domains. Western Corsica consists largely of stable Hercynian basement characterized by ZFT ages in the range 161–114 Ma. We interpret these ages (Late Jurassic–Early Cretaceous) as the product of a long-lived Tethyan thermal event related to continental rifting and subsequent drifting during the separation of the European and African plates and the formation of the Liguro–Piemontese ocean basin. In contrast to Hercynian Corsica, Alpine Corsica (northeast Corsica) experienced widespread deformation and metamorphism in Late Cretaceous(?)–Tertiary time. Dated samples from Alpine Corsica range in age from 112 to 19 Ma and all are reset or partially reset by one or more Alpine thermal events. The youngest ZFT grain ages are from the northernmost Alpine Corsica and define an age population at ~24 Ma that indicates cooling after Tertiary thermal events associated with the Alpine metamorphism and the opening of the Liguro–Provençal basin. A less well-defined ZFT age population at ~72 Ma is present in both Alpine Corsica and Hercynian basement rocks. The thermal history of these rocks is not clear. One interpretation is that the ZFT population at ~72 Ma reflects resetting during a Late Cretaceous event broadly synchronous with the early Alpine metamorphism. Another interpretation is that this peak is related to variable fission-track annealing and partial resetting during the Tertiary Alpine metamorphic event across central to north-eastern Corsica. This partial age resetting supports the presence of a fossil ZFT partial annealing zone and limits the peak temperature in this area below 300 °C, for both the affected pre-Alpine and Alpine units.

Keywords: Thermochronology; Fission-track annealing; High-pressure metamorphism; Cenozoic; Corsica

1. Introduction

Fission-tracks (FT) in zircon have an effective closure temperature of ~ 240±30 °C in natural systems (Hurford, 1986; Brandon et al., 1998; Tagami et al.,

* Corresponding author. Dipartimento di Scienze della Terra e Geologico-Ambientali, Alma Mater Studiorum — Università di Bologna, Via Zamboni 67, 40126 Bologna, Italy.
E-mail address: fellin@geomin.unibo.it (M.G. Fellin).

0040-1951/$ - see front matter © 2006 Elsevier B.V. All rights reserved.
doi:10.1016/j.tecto.2006.05.001

1998; Brix et al., 2002). The closure temperature of the ZFT system serves as a useful thermochronologic reference to unravel the long-term exhumation history of convergent mountain belts. The rocks of most orogenic belts have relatively well-defined FT cooling patterns that can be related to exhumation driven by tectono-thermal events. One interesting situation is when cooled zircons with different ages and variable internal radiation damage are affected by low-temperature thermal perturbations. In these cases, heterogeneous annealing and partial annealing result in scattered grain-age distributions even in plutonic rocks where all grains should have experienced the same thermal history. In these cases, slight differences in the single-grain concentration of U+Th results in minor variation in radiation damage, which then affects annealing kinetics (Garver et al., 2005). This annealing effect is best seen in orogenic belts that have experienced multiple tectono-thermal events, or a thermal perturbation.

A portion of the Alpine orogenic belt is exposed on the island of Corsica, a continental block located in the Western Mediterranean. Corsica comprises a pre-Alpine basement (Hercynian Corsica) to the south-west, and metamorphic rocks (Alpine Corsica) to the north-east (Fig. 1). In south-western Corsica, our ZFT dating can be used to determine to what extent the Hercynian basement has been affected by an Alpine thermal

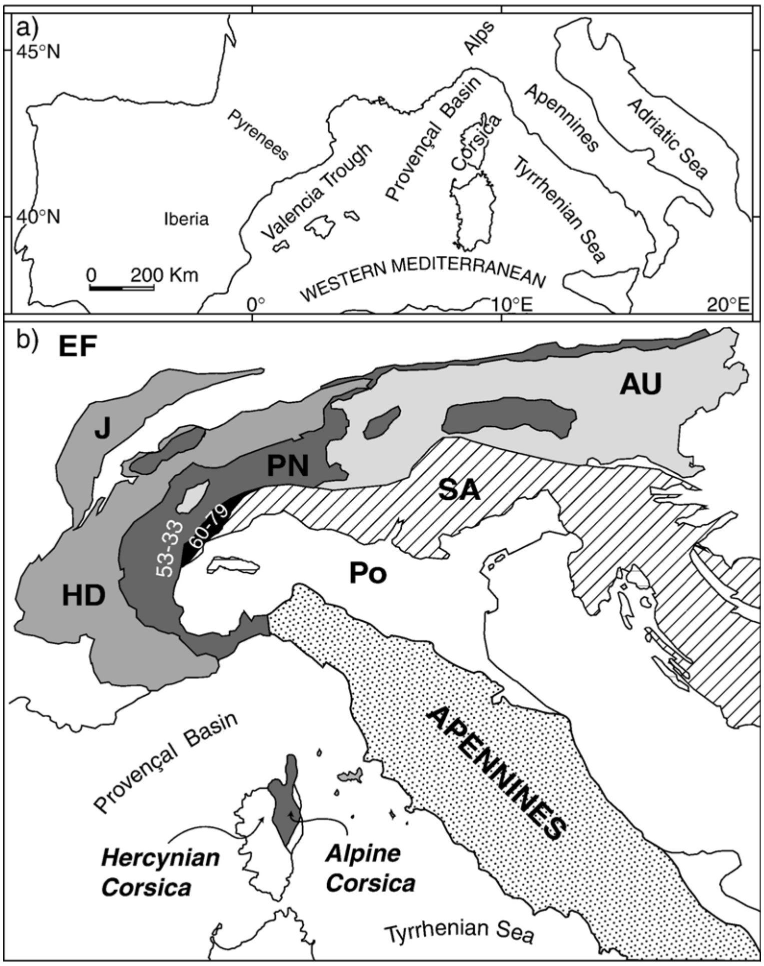

Fig. 1. a) Location map of Corsica; b) map of the Alps–Apennines orogenic system and main tectonic boundary between the Alpine and pre-Alpine (Hercynian) units of Corsica. 53–33 and 60–79 indicate the age (Ma) of the high-pressure, low-temperature metamorphic rocks of the Piemonte zone and of the Sesia Lanzo zone and in the Western Alps, respectively (e.g. Rubatto et al., 1999; Dal Piaz et al., 2001; Agard et al., 2002 and references therein). Abbreviations as follows: J — Jura; EF — European Foreland basin; HD — Helvetic Domain; PN — Penninic Nappes; Po — Po basin (foreland basin); AU — Austral-Alpine units; SA — Southern Alps.

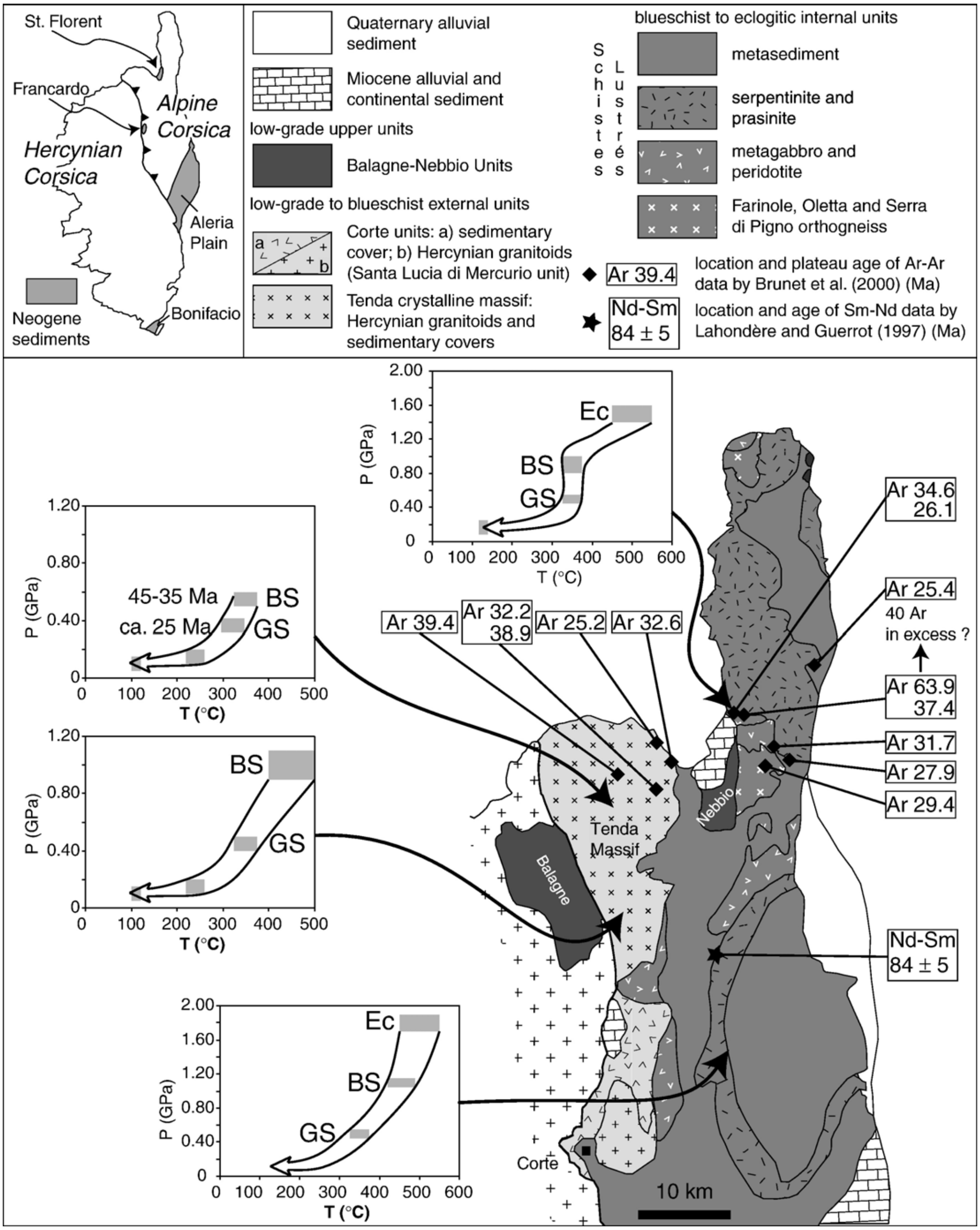

Fig. 2. Geological sketch map of northeastern Corsica modified after Daniel et al. (1996) with pressure–temperature paths (see text for references), ^{40}Ar–^{39}Ar on white mica and Sm–Nd ages of the Alpine units.

overprint. In northeastern Corsica, our primary goal is to better constrain the time of cooling following Alpine high-pressure metamorphism. The age of this metamorphism remains uncertain because existing chronological data point to either a Late Cretaceous age (84±5 Ma, Lahondère and Guerrot, 1997) and/or to a Middle-to-Late Eocene age (45–35 Ma, Brunet et al., 2000). Finally, our study also supplements the FT dating by Lucazeau and Mailhé (1986) and Mailhé et al. (1986). These authors report FT ages from Corsica on both apatite and zircon. Additional apatite FT age determinations were published later (Cavazza et al., 2001; Zarki-

Jakni et al., 2004; Fellin et al., 2005a) and demonstrate that the apatite dating by Lucazeau and Mailhé (1986) are problematic.

Our results have important implications for the interpretation of ZFT ages in metamorphic rocks that have experienced a low-temperature thermal overprint (~300 °C). In agreement with previous studies (Brix et al., 2002; Garver et al., 2005), we have found that the ZFT annealing behavior is sensitive not only to temperature and cooling rate, but also to radiation damage in zircon. In this paper, we address the problem of the age and conditions of the Alpine metamorphic event in Corsica and of the interpretation of ZFT data. We first review the petrologic and chronologic evidence from previous studies, and possible evolutionary models for Corsica in the context of the Alpine–Apennine orogenic system, then we present the new ZFT ages and discuss their implications.

2. Geological setting

2.1. Main geological units of Corsica: conditions and age of metamorphism

Northeastern Corsica, commonly termed Alpine Corsica because of its geologic similarity to the Western Alps, consists of a nappe pile thrust onto the pre-Alpine basement exposed in western and southern Corsica (Fig. 2). The pre-Alpine Hercynian basement consists of Carboniferous to Early Permian granitoids (260–345 Ma), pre-Hercynian metamorphic host rocks and Permian volcanic rocks (e.g. Rossi and Cocherie, 1991; Gattacceca et al., 2004). These crystalline rocks are overlain by Triassic to Paleocene continental and marine sedimentary rocks and by Eocene foredeep strata (e.g. Durand-Delga, 1984). The Triassic to Paleocene sedimentary rocks were deposited on the Hercynian basement when Hercynian Corsica was part of the western passive margin of the Alpine Tethys (e.g. Dal Piaz et al., 1977; Stämpfli and Marchant, 1998). Alpine deformation within the Hercynian basement occurred along NE-trending ductile shear zones with strike-slip kinematics, and along the NS-trending contact with the Alpine metamorphic units (Maluski et al., 1973). Next to the contact between Alpine and pre-Alpine rocks, granites were deformed into orthogneisses locally bearing blue amphibole and stilpnomelane that developed at the expense of green alkaline amphibole (Amaudric du Chaffaut and Saliot, 1979; Rossi et al., 1994). This mineral assemblage reflects intermediate pressure conditions, which are Eocene in age based on ^{40}Ar–^{39}Ar ages on K-feldspar (Maluski, 1977a,b).

Alpine Corsica consists of metamorphosed Jurassic ophiolites and their sedimentary cover imbricated with slices of Hercynian basement. Metamorphic grade generally increases eastward with greenschist to blueschist facies in the western external units, and blueschist to eclogitic facies in the eastern internal units (Gibbons and Horak, 1984; Warburton, 1986; Caron and Pequignot, 1986; Lahondère, 1991).

The main units of Alpine Corsica are (Fig. 2): (i) the low-grade metamorphic Balagne–Nebbio units; (ii) the intermediate to high-grade continental rocks of Corte; (iii) the Tenda massif; (iv) the high-pressure units including the Farinole and Oletta–Serra di Pigno orthogneiss; and (v) the oceanic Schistes Lustrés *sensu lato* (herein Schistes Lustrés).

i) The Balagne–Nebbio units are mostly Jurassic oceanic rocks and Cretaceous to Eocene foredeep strata metamorphosed under very low grade conditions ($P<0.5$ GPa, $T<350$ °C) (Nardi et al., 1978; Amaudric du Chaffaut and Saliot, 1979; Durand-Delga, 1984; Dallan and Puccinelli, 1986; Saccani et al., 2000; Padoa et al., 2002). During the Middle to Late Eocene, the Balagne–Nebbio units were thrust westward onto the Corsican HP units and onto the foreland strata, which overlie the Hercynian basement (Durand-Delga, 1984).
ii) The Corte units form a steeply dipping imbricate stack of thrust sheets between the Hercynian basement and the HP Alpine units. They comprise slices of Hercynian basement, as well as Mesozoic and Eocene sedimentary rocks that are overridden by low-grade metamorphic Alpine units, and later back-thrust above the HP Alpine units (Durand-Delga, 1984; Saccani et al., 2000; Peybernès et al., 2001). These units were variably deformed during greenschist facies metamorphism and blue amphibole (crossite, Mg-riebeckite) locally developed in the high-strain shear zones (Amaudric du Chaffaut and Saliot, 1979; Bézert and Caby, 1988). This mineral assemblage limits the maximum pressure to 0.5 GPa at a temperature of 300 ± 50 °C (Lahondère, 1991). Peak metamorphism in the Corte units post-dates Bartonian nummulites (40–37 Ma) in a conglomerate that has developed blue amphibole. In addition, a ^{40}Ar–^{39}Ar age of 40.0 ± 2.0 Ma was determined for a blue amphibole in a basement slice near Corte (Amaudric du Chaffaut and Saliot, 1979). Apatite FT ages of ca. 30 Ma indicate cooling below 110 °C of the Corte nappe stack during the Early Oligocene (Fellin et al., 2005a).

iii) The Tenda crystalline massif is a fault-bounded antiformal high between the Hercynian basement on the west, and the HP Alpine units on the east. The massif consists mainly of Hercynian granitoid basement with its volcanic and sedimentary cover. In the northeastern and southern sectors of the massif, the granitoid rocks are metamorphosed to orthogneiss, and show high-strain shear zones with locally developed epidote-blueschist facies mineral assemblages. Peak pressures and temperatures of 1.0±0.1 GPa and 300–500 °C have been estimated for this metamorphism (Tribuzio and Giacomini, 2002). These conditions are higher than previous estimates of 0.5 Gpa and 300±50 °C (Lahondère, 1991; Jolivet et al., 1998). Both studies conclude that the geothermal gradient in the Tenda massif during overthrusting was very low (10–13 °C/km). The Tenda orthogneisses typically display greenschist facies metamorphism associated with an early stage of syncontractional exhumation (Waters, 1990; Molli and Tribuzio, 2004), and pervasive retrograde metamorphism related to late orogenic extensional exhumation (Jolivet et al., 1990, 1991, 1998, Brunet et al., 2000).
^{40}Ar–^{39}Ar plateau ages on phengites from rocks of the northern Tenda massif demonstrate cooling from temperatures greater than 350 °C between 39 and 25 Ma (Brunet et al., 2000) (Fig. 2). Brunet et al. (2000) interpret the ^{40}Ar–^{39}Ar age spectra of these samples as indicating phengite crystallization between 45 and 35 Ma. However, peak temperature during the HP event is poorly constrained by the thermobarometry and therefore it is uncertain whether the ^{40}Ar–^{39}Ar data by Brunet et al. (2000) represent crystallization ages or cooling ages. In the latter case they would constrain only a minimum age for the peak HP event.

iv) The Farinole and Oletta–Serra di Pigno orthogneiss are low-temperature and high-pressure units consisting of continental slices interleaved with the Schistes Lustrés during the early and deep orogenic deformation stages (Waters, 1990). Maximum burial depths are recorded by the Farinole orthogneiss that bear mineral assemblages reflecting eclogitic facies conditions of 1.5 Gpa and 500±50 °C overprinted by retrogression to an intermediate blueschist facies stage and finally to greenschist facies conditions (0.5 Gpa and 350 °C) (Lahondère, 1991). Phengite ^{40}Ar–^{39}Ar plateau ages of 63.9 and 37.4 Ma have been determined in the Farinole HP orthogneiss, but the older age is likely due to excess Ar (Brunet et al., 2000) (Fig. 2). The ages between 37 and 26 Ma for phengites are associated with cooling during the exhumation that post-dates HP metamorphism.

v) The Schistes Lustrés are named after the Schistes Lustrés of the Piemonte zone of the Western Alps. They are Jurassic oceanic rocks and their Jurassic-to-Cretaceous sedimentary cover metamorphosed to eclogite and blueschist facies. Pressure and temperature conditions for the eclogite facies rocks correspond to 1.8 GPa and 500±50 °C (Caron and Pequignot, 1986; Lahondère, 1991). Estimates of the peak metamorphic conditions for the blueschist facies rocks are 1.1±0.05 GPa and 455±35 °C for the metabasites (Lahondère, 1991) and 1.4–1.7 Gpa and 300–380 °C for the metapelites (Jolivet et al., 1998). Together these units record a complex deformation history consisting of two main events (Cohen et al., 1981; Mattauer et al., 1981; Gibbons and Horak, 1984; Warburton, 1986; Jolivet et al., 1990, 1991; Caron, 1994; Daniel et al., 1996; Jolivet et al., 1998; Brunet et al., 2000): (i) a first episode of Late Cretaceous–Eocene early tectonic burial and metamorphism followed by thrusting and backthrusting deformations along with syncontractional exhumation, (ii) a second episode that involved widespread pervasive retrogression under greenschist-facies conditions and related extensional exhumation. The HP metamorphism in these units predates Eocene sandstone (Prunelli Flysch), which unconformably overlies both the Hercynian basement and the Schistes Lustrés. A four point Sm–Nd date on whole rock in an ophiolite-derived eclogite yields an internal isochron of 84±5 Ma (Lahondère and Guerrot, 1997).

2.2. Oliogocene to Miocene tectonic evolution of Corsica

In the Early Oligocene, the tectonic contacts between the Schistes Lustrés and the Balagne–Nebbio units, and between Alpine and Hercynian Corsica were reactivated as ductile-to-brittle extensional faults that reversed the sense of the earlier thrust displacement (Daniel et al., 1996; Jolivet et al., 1998; Brunet et al., 2000) (Fig. 3). The extensional reactivation of the contact between Alpine and Hercynian Corsica led to uplift and exhumation of its footwall rocks, which is the Hercynian basement, where an Oligocene thermal overprint is

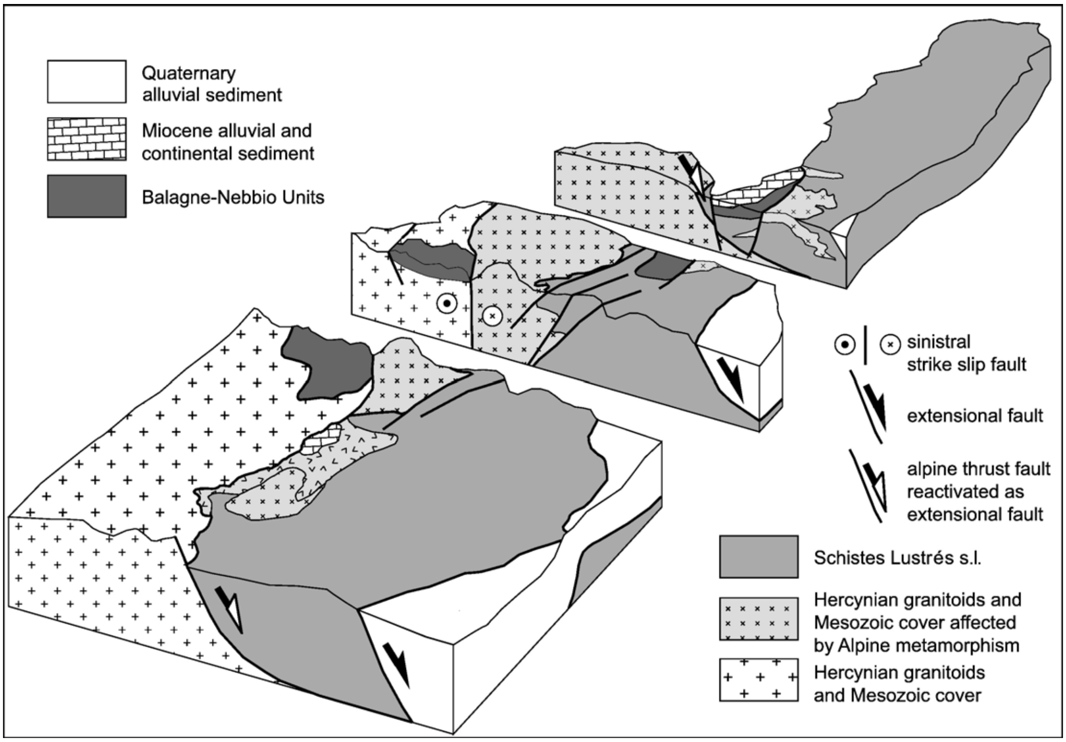

Fig. 3. Block diagram showing the geometry and dynamics of the main tectonic boundaries of northeastern Corsica (modified after Jolivet et al., 1998). During the Oligocene–Miocene, the main Alpine west-vergent thrusts have been reactivated as extensional ductile-to-brittle faults (Daniel et al., 1996; Jolivet et al., 1991, 1998) and as transpressional faults (Waters, 1990; Lahondère et al., 1999).

recorded by apatite FT ages (Zarki-Jakni et al., 2004). In eastern Corsica, extensional reactivation of the Alpine contacts was accompanied by extensional exhumation and widespread retrogression under greenschist to brittle conditions between 35 and 25 Ma.

Late Oligocene-to-Middle Miocene rifting and final formation of the Provençal–Ligurian basin are associated with counterclockwise rotation of the Corsica–Sardinia block away from Europe (Vigliotti and Langenheim, 1995), and with calcalkaline andesitic volcanic activity along the western margin of Corsica (e.g. Ottaviani-Spella et al., 1996; Rollet et al., 2002). During this rotation, the contact between Alpine and Hercynian Corsica was locally reactivated as a left-lateral transpressional wrench zone that had splays along the western and eastern Tenda margins (Waters, 1990; Lahondère et al., 1999). Transpressional deformation was followed in the Early and Middle Miocene by extensional brittle deformations resulted in the formation of shallow marine basins (Orszag-Sperber and Pilot, 1976; Cubells et al., 1994; Ferrandini et al., 1998; Mauffret and Contrucci, 1999; Fellin et al., 2005a). By the Middle Miocene, all Alpine units and Hercynian basement had cooled below 70 °C as indicated by FT and U–Th/He ages on apatite (Cavazza et al., 2001; Zarki-Jakni et al., 2004; Fellin et al., 2005a, b) (Fig. 3).

During Late Miocene inversion of the Corsica shallow-water basins (Fellin et al., 2005a) is followed by renewed extension accompanied by flexural uplift and kilometer-scale folding (Orszag-Sperber and Pilot, 1976; Conchon, 1977; Durand-Delga, 1984). Finally, contractional deformation is locally recorded in the Pleistocene to Quaternary marine and continental sedimentary rocks in the eastern Corsican plains (Fellin et al., 2005a).

2.3. *High-pressure metamorphism and evolutionary models for Alpine Corsica*

The available chronological data broadly place HP metamorphism in Corsica in the interval Late Cretaceous–Late Eocene. The HP metamorphism in the northeastern Tenda massif (Brunet et al., 2000) is inferred to be Middle to Late Eocene based on ^{40}Ar–^{39}Ar data on white mica. In the Corte nappe stack, meta-conglomerates containing Bartonian nummulites (Bézert and Caby, 1988) and apatite FT ages

(Fellin et al., 2005a; Fig. 4) constrain the metamorphic event in a short time interval during the Late Eocene–Early Oligocene (between ca. 40–37 Ma and 30 Ma). The age of the HP event in the Schistes Lustrés is older than Eocene because foredeep sandstones (Prunelli Flysch) unconformably overlie the Schistes Lustrés and the Hercynian basement. An 84±5 Ma Sm–Nd date from the metabasites of the Schistes Lustrés indicates a Late Cretaceous age for the eclogitic metamorphic event (Lahondère and Guerrot, 1997). The Late Eocene–Middle Oligocene ^{40}Ar–^{39}Ar ages on phengites from the eclogitic-facies Farinole orthogneiss are cooling ages that yield only a minimum age for the HP event (Brunet et al., 2000). The Late Cretaceous Sm–

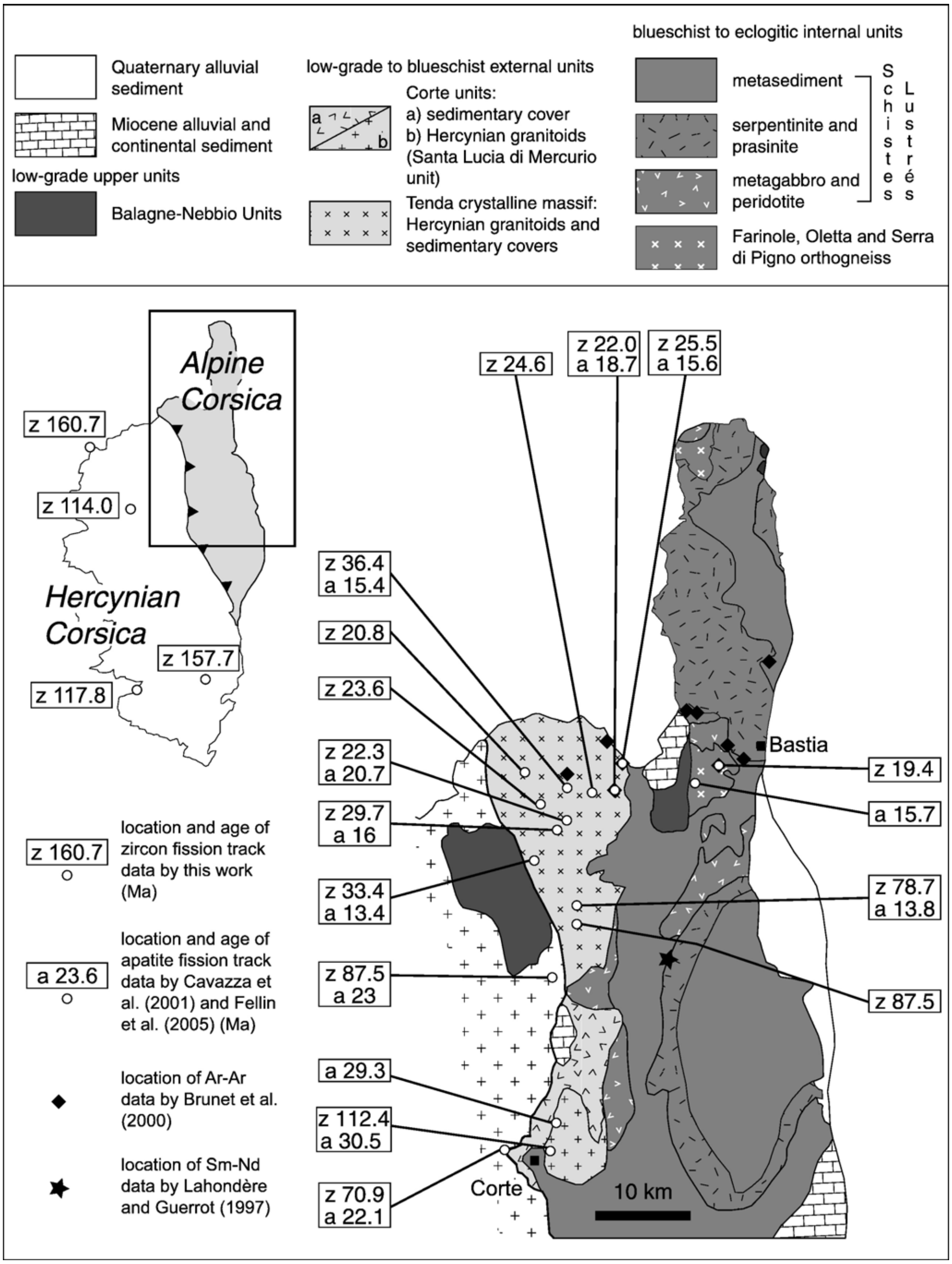

Fig. 4. Geological sketch map of northeastern Corsica modified after Daniel et al. (1996) with our zircon fission-track data and apatite fission-track data from Cavazza et al. (2001) and Fellin et al. (2005a). Fission-track ages shown are all central ages.

Nd age for the eclogitic event is an isolated datum that has not been confirmed by further data, nevertheless some previous studies (e.g. Malavieille et al., 1998; Rossi et al., 2001) point out that this Late Cretaceous age is comparable to the age of the eclogitic rocks of the Sesia–Lanzo Zone [Western Alps, 65–76 Ma (Rubatto et al., 1999)] implying a similar early Alpine burial history for these two areas. Phengites from the Schistes Lustrès (*s.s.*) of the Western Alps yield ^{40}Ar–^{39}Ar ages between 35.5 and 53.7 Ma (Agard et al., 2002).

A Cretaceous age for the peak HP metamorphism would imply that this event occurred within the Alpine orogenic system, which was characterized by a south-dipping subduction polarity (or east-dipping with respect to the present location of Corsica). In this scenario, contractional deformation and HP metamorphic conditions that affected eastern Corsica during the Eocene occurred after a reversal in subduction polarity from east-dipping to west-dipping related to the onset of the Apenninic accretion phase (e.g. Boccaletti et al., 1971; Mattauer and Proust, 1976; Durand-Delga, 1984; Molli and Tribuzio, 2004 and references therein). Alternatively, the ^{40}Ar–^{39}Ar data and the stratigraphic constraints in the Corte unit point to an Eocene age for the peak HP metamorphic event. In this scenario, the formation of the Corsican nappe could have developed as back-thrusting in the retro-wedge of the west-dipping Apenninic subduction system (Treves, 1984; Principi and Treves, 1984; Rossi et al., 2001). Nevertheless, the timing of these alternative evolution models is a rather complex issue especially in light of the most recent dating in the Western Alps indicating that all the HP units except for the Sesia–Lanzo Zone underwent HP metamorphism during the Late Paleocene to Eocene (e.g. Dal Piaz et al., 2001).

3. Zircon fission-track

3.1. Sample preparation

The dated zircons were all separated from granitoid basement rocks. Bulk rock samples were first crushed and pulverized with a disk mill. Zircons were separated from the washed and sieved pulverized samples using standard heavy-liquid and magnetic separation techniques (Naeser, 1976). The zircons were mounted in Teflon discs and then polished to expose internal zircon surfaces. The mounted zircons were incrementally etched for 1.5 to 6 h in a NaOH–KOH eutectic melt at 220 °C. In many separates a high proportion of the zircons proved to be metamict and did not etch well. Accordingly, the samples were cleaned up by hand-picking the clearer euhedral crystals and discarding turbid and opaque material. In the four dated samples from Hercynian Corsica only few grains were countable and were given a short etch of 1.5 to 3 h. In contrast to these samples from the Hercynian basement, dated zircons from most Alpine Corsica samples etch well yielding more countable grains that were given etch times up to 6 h.

All mounts were irradiated at the Oregon State University reactor, along with SRM962 or CN5 glass and Fish Canyon Tuff zircon standards (Hurford, 1990). FT ages were calculated for each sample using the ζ method: ζ values and FT central ages are listed in Table 1.

Samples were processed and irradiated in three different runs over 4 years and during this time laboratory procedures underwent some modifications. Because of these changes, the FT ages were calculated using individual ζ values for each of the three irradiations. The individual ζ values were determined using two standard mounts per irradiation, and the variable ζ values obtained reflect the use of different glass standard and varying neutron fluence.

3.2. Annealing of zircon fission-tracks

The annealing kinetics of FT in zircon and the temperature limits of the partial annealing zone (PAZ) vary as a function of heating and cooling rates, and of radiation damage in zircon (Brandon et al., 1998; Brix et al., 2002; Rahn et al., 2004; Garver et al., 2005). For heating duration of 5–10 Myr, extrapolations from laboratory data to geological time-scale and deep borehole data constrain the lower temperature limit of the PAZ for zircon at ~ 200 °C (Yamada et al., 1995; Tagami et al., 1996; Tagami and Shimada, 1996; Tagami et al., 1998). Nevertheless, as discussed by Garver et al. (2005), this lower temperature bound for the PAZ is possibly overestimated due to the small window for etch times used in these experiments. The temperature of complete resetting for radiation-damaged zircons has not been measured in deep boreholes but it has been extrapolated in natural settings from cooling paths of fully reset zircons (Brandon et al., 1998). In these natural settings fully reset, radiation-damaged zircons indicate annealing limits of 180 °C and 240 °C for 10 Myr heating events. For short duration heating events of 4±2 Myr, studies on zircons with little or no radiation damage in fossil annealing zones of high-grade metamorphic terrains yield estimates for the total annealing temperature as high as 350–400 °C (Brix et al., 2002).

Table 1
Zircon FT data

n	Sample	Unit	Elevation (m)	UTM coordinate (Zone 32) Easting (m)	UTM coordinate (Zone 32) Northing (m)	No. of grains	ρ_d (tracks/cm^{-2})	ρ_s (tracks/cm^{-2})	N_s	ρ_i (tracks/cm^{-2})	N_i	P (χ^2) (%)	Central age	-2σ	$+2\sigma$	Local ζ-CN5
1	V706	Oletta–Serra di Pigno orthogneiss	150	529,750	4,722,550	10	1.435E+05	5.433E+06	1650	6.901E+06	2096	0.3	19.4	2.5	2.9	344.08±16.02
2	V705	Orthogneiss of the Tenda crystalline massif (Lama Unit)	300	512,725	4,733,250	8	1.436E+05	6.730E+06	1281	7.964E+06	1516	0.1	20.8	3.1	3.6	344.08±16.02
3	TE09	Orthogneiss of the Tenda crystalline massif (Monte Genova Unit)	25	522,625	4,725,950	9	1.235E+05	4.605E+06	1118	4.963E+06	1205	12.3	25.5	3.1	3.5	445.51±18.12
4	TE26	Orthogneiss of the Tenda crystalline massif (Monte Genova Unit)	295	517,150	4,723,450	9	1.230E+05	7.464E+06	1326	5.921E+06	1052	0.1	36.4	5.3	6.2	473.52±18.07
5	TE27	Orthogneiss of the Tenda crystalline massif (Monte Genova Unit)	250	519,000	4,723,100	7	1.225E+05	9.929E+06	966	1.100E+07	1070	47.6	24.6	2.8	3.2	445.51±18.12
6	TE28	Orthogneiss of the Tenda crystalline massif (Monte Genova Unit)	220	520,400	4,722,675	6	1.230E+05	5.598E+06	592	7.565E+06	800	0.3	22.0	3.9	4.8	473.52±18.07
7	TE25	Orthogneiss of the Tenda crystalline massif (Lama Unit)	340	513,750	4,722,425	7	1.228E+05	7.920E+06	871	9.147E+06	1006	27.1	23.6	2.9	3.3	445.51±18.12
8	TE85	Orthogneiss of the Tenda crystalline massif (Lama Unit)	555	517,120	4,721,170	6	1.200E+05	6.951E+06	541	8.788E+06	684	10.2	22.3	3.3	3.8	473.52±18.07
9	TE84	Orthogneiss of the Tenda crystalline massif (Lama Unit)	515	516,260	4,720,250	6	1.200E+05	9.760E+06	611	9.169E+06	574	0.9	29.7	5.4	6.7	473.52±18.07
10	TE79	Orthogneiss of the Tenda crystalline massif (Lama Unit)	630	514,600	4,717,370	7	1.210E+05	1.157E+07	793	9.923E+06	680	0.9	33.4	5.5	6.5	473.52±18.07
11	TE31	Orthogneiss of the Tenda crystalline massif (Monte Asto Unit)	1509	517,800	4,713,580	10	1.220E+05	2.191E+07	2428	7.507E+06	832	0.5	78.7	10.7	12.4	445.51±18.12
12	TE32	Orthogneiss of the Tenda crystalline massif (Monte Asto Unit)	1245	517,875	4,712,400	6	1.219E+05	2.353E+07	1513	7.201E+06	463	6.4	87.5	13.0	15.3	445.51±18.12
13	TE76	Granitoid of the Corte Units (Santa Lucia di Mercurio Unit)	365	514,370	4,683,400	6	1.210E+05	2.921E+07	1112	7.381E+06	281	94.7	112.4	15.9	18.4	473.52±18.07
14	TE73	Hercynian granitoid (Castirla)	370	511,170	4,692,170	6	1.220E+05	2.684E+07	999	8.221E+06	306	5.8	87.5	13.0	15.3	473.52±18.07
15	TE77	Hercynian granitoid (Corte)	470	511,770	4,682,370	5	1.210E+05	1.697E+07	689	6.821E+06	277	36.4	70.9	10.5	12.3	473.52±18.07
16	V704	Hercynian granitoid (Calvi)	35	480,541	4,713,024	6	1.438E+05	2.000E+07	1320	3.061E+06	202	3.7	160.7	32.7	40.8	344.08±16.02
17	V702	Hercynian granitoid (Col de Vergio)	1100	492,503	4,682,106	8	1.439E+05	1.992E+07	1938	4.286E+06	417	34.0	114.0	15.2	17.3	344.08±16.02
18	V699	Hercynian granitoid (Col de Bavella)	1215	518,630	4,627,140	10	1.445E+05	1.500E+07	2272	2.338E+06	354	30.5	157.7	22.0	25.5	344.08±16.02
19	V700	Hercynian granitoid (Propriano)	40	493,181	4,611,515	10	1.442E+05	1.525E+07	2736	3.189E+06	572	0.0	117.8	21.7	26.6	344.08±16.02

Central ages calculated using dosimeter glass CN5 and the ζ-CN5 reported in the table (zircon fission-track data). The variable values of ζ-CN5 reflect variation through time of the ζ value. ρ_s, spontaneous track densities measured in internal mineral surfaces; Ns, total number of spontaneous tracks; ρ_i and ρ_d, induced and dosimeter track densities on external mica detectors (g=0.5); Ni and Nd, total numbers of racks; $P(\chi^2)$, probability of obtaining χ^2 value for y degrees of freedom (where y=number of crystals−1); a probability of 5% is indicative of a homogeneous population.

The annealing temperature bounds are sensitive not only to heating/cooling rate but also to the degree of radiation damage in individual zircons (Garver and Kamp, 2002; Rahn et al., 2004; Garver et al., 2005). In cases of high-radiation damage, zircons may be reset at temperatures as low as 180–200 °C whereas in cases of low-radiation damage zircons appear to be fully reset at temperatures in excess of ~ 280–300 °C. The degree of radiation damage is a function of the uranium and thorium content of zircons and of the time elapsed since onset of cooling. Even totally annealed zircons from a single source (e.g. a plutonic rock) may show scattered grain-age distributions that result from heterogeneous radiation damage and therefore variable track retentivity (e.g. Fig. 5) (Garver et al., 2005). Because of the variable retentivity of zircons, ZFT samples commonly consist of multiple grain-age populations with the older populations comprising high-retentive zircons commonly with a low U+Th content, and the younger populations comprising low-retentive zircons commonly with a high U+Th content. Thus, not only partially annealed samples but also fully reset samples may show chi-square (χ^2) values lower than 5% and fail the χ^2 test, which is used to determine whether a sample consists of a single grain age population (see Galbraith, 1981). In cases of widely scattered zircon grain ages that fail χ^2 (or "over-dispersed" grain ages), the central age for ZFT samples is not representative of cooling because zircons trace the long thermal evolution of the source rock and only the low-retentive zircons are likely to record the youngest thermal event. In fact, in over-dispersed samples, a mean age or a central age is virtually meaningless and masks potentially useful structure in the age data. To examine the heterogeneous annealing of the ZFT samples and its significance in terms of thermal evolution, a more suitable approach is the analysis of the zircon grain-age distribution through the binomial peak-fitting method (Brandon, 1996; Garver et al., 2005, Locke and Garver, 2005). This statistical method is based on the bimodal distribution and it decomposes the observed grain-age distribution into grain-age components.

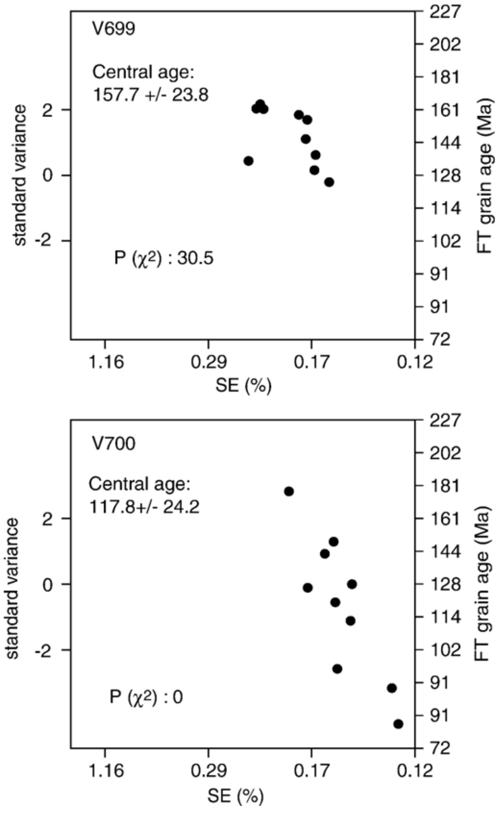

Fig. 5. Radial plots of the zircon fission-track (ZFT) grain ages of two samples from the Hercynian granitoids of Western Corsica. These plots show the wide variation range of ZFT grain ages in samples consisting of a single-source plutonic rock. A wide variation range of ZFT grain ages is shown also by the sample with a high chi-squared values ($P(\chi^2)=30.5$). These data illustrate the challenge of interpreting ZFT grain ages from samples that have been affected by multiple heating/cooling events. The difference in grain ages is inferred to have been caused by variable track retention, which is affected by internal radiation damage.

3.3. Zircon fission-track results

In this section we review ZFT ages systematically across the study area. Six samples for FT dating were collected in Hercynian Corsica and thirteen in Alpine Corsica (Fig. 4, Table 1). Four samples from the Hercynian granitoids in Western Corsica show ZFT ages ranging between 161 and 114 Ma, whereas two samples from the same rocks exposed near to the Alpine contact have ZFT ages of 88 and 71 Ma.

ZFT samples from Alpine Corsica were collected in the Corte units, the Tenda massif and the Oletta–Serra di Pigno units. All these units consist of Hercynian granitoids and differ in the grade of Alpine metamorphism. ZFT ages from these units range between 112 and 19 Ma and these ages become progressively younger from south to north (Figs. 4 and 6a). In the south, the Corte units have the oldest ZFT age of 112 Ma. In the southern Tenda massif, two samples yield ZFT ages of 88 and 79 Ma. Finally, the northern Tenda massif and the Oletta–Serra di Pigno units have ZFT ages between 36 Ma and 19 Ma.

Our results are partly similar to the determinations by Mailhé et al. (1986) who determined ages between 225 and 110 in the Hercynian basement of western Corsica, and of ~60–70 Ma in the Hercynian basement next to

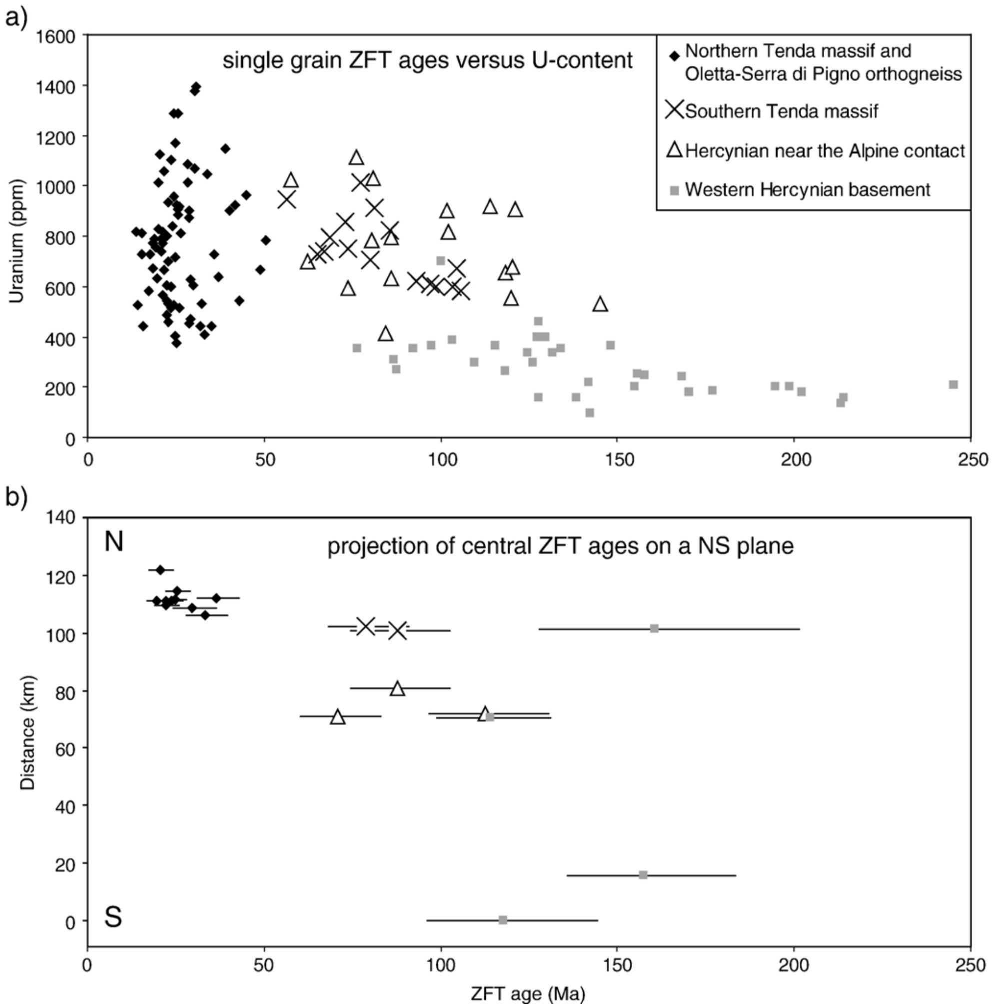

Fig. 6. a) Projection on a N–S vertical plane of zircon fission-track (ZFT) central ages (±2σ) from the Corte region and the Tenda massif. b) Plot of the Corsica ZFT ages versus uranium+thorium content (U) determined on the basis of the induced fission tracks. This diagram shows that younger ZFT ages tend to occur in zircons with a high U content. U-rich zircons generally show high radiation damage, low fission-track retentivity and therefore a low annealing temperature.

the Alpine contact and in the southern Tenda massif. However, Mailhé et al. (1986) did not report ZFT ages younger than 36 Ma as we did find in the northern Tenda and Oletta–Serra di Pigno units. It is quite possible that this difference results from different etching conditions used in either lab. Apatite FT ages by Mailhé et al. (1986) are also much older than the ages determined by later studies (Cavazza et al., 2001; Zarki-Jakni et al., 2004; Fellin et al., 2005a). This indicates that FT data by Mailhé et al. (1986) on both apatite and zircon may be affected by a common methodological bias.

We could date only five to ten zircon grains for each sample due to the paucity of well-etched, countable grains. Nine out of nineteen samples fail the χ^2 test, which indicates overdispersion almost certainly related to partial annealing and variable track retentivity. Partial annealing conditions can be tested by taking into account further constraints on the thermal history of the rock as discussed in the following section. Variable retentivity in zircon can be tested by analyzing U content derived from the induced track density given that zircon retentivity is controlled chiefly by U content (and Th to a lesser degree) and time (Garver et al., 2005). The relation between ZFT ages and U content is shown by Fig. 6b, which illustrates two points. The first is that younger ZFT ages occur in grains with a higher U content. This direct relation between U content and ZFT age has been observed also in other studies, both in detrital and single-source zircon grains, and is related to the selection of etchable and countabe zircons, and/or preferential resetting of high-damage grains (Garver et al., 2005; Bernet and Garver, 2005). A selection of

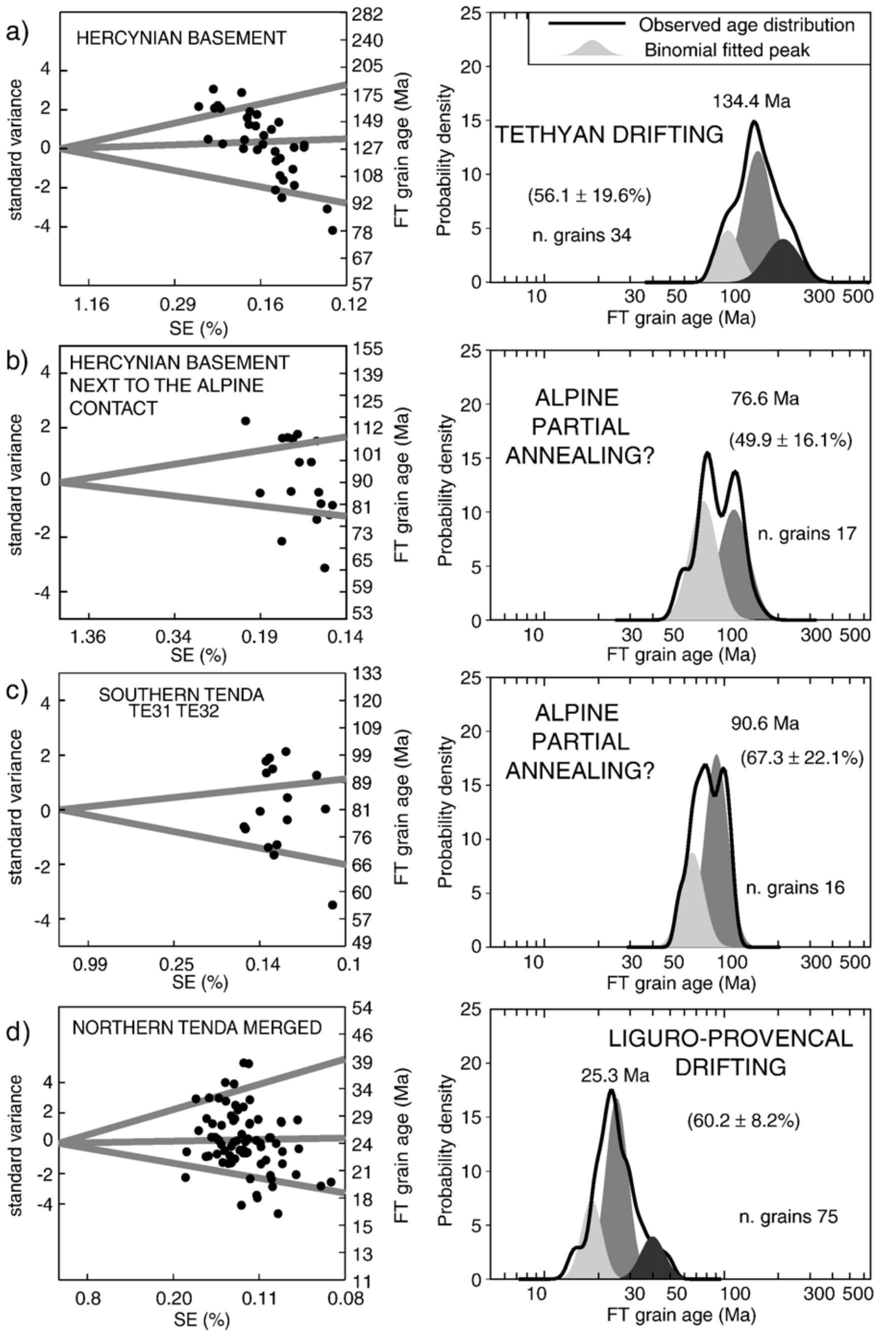

Fig. 7. Results from binomial peak-fitting (Brandon, 1996) represented through the radial (left column) and probability density plots (right column). On these plots, the observed distribution is reported together with the individual peaks representing the grain-age components. On the radial plots, zircon fission-track (ZFT) grain ages are represented by dots and the individual peaks by the gray lines. On the probability density plots black solid lines represent the observed grain-age distribution, and grey areas represent the individual peaks. a) ZFT grain ages from four samples from the Hercynian basement of Western Corsica. b) ZFT grain ages from two samples from the Hercynian granitoids, located next to the Alpine contact and affected by Alpine metamorphism. c) ZFT grain ages from two samples from the southern Tenda massif. d) Grain ages from samples from the northern Tenda massif and the Oletta–Serra di Pigno units.

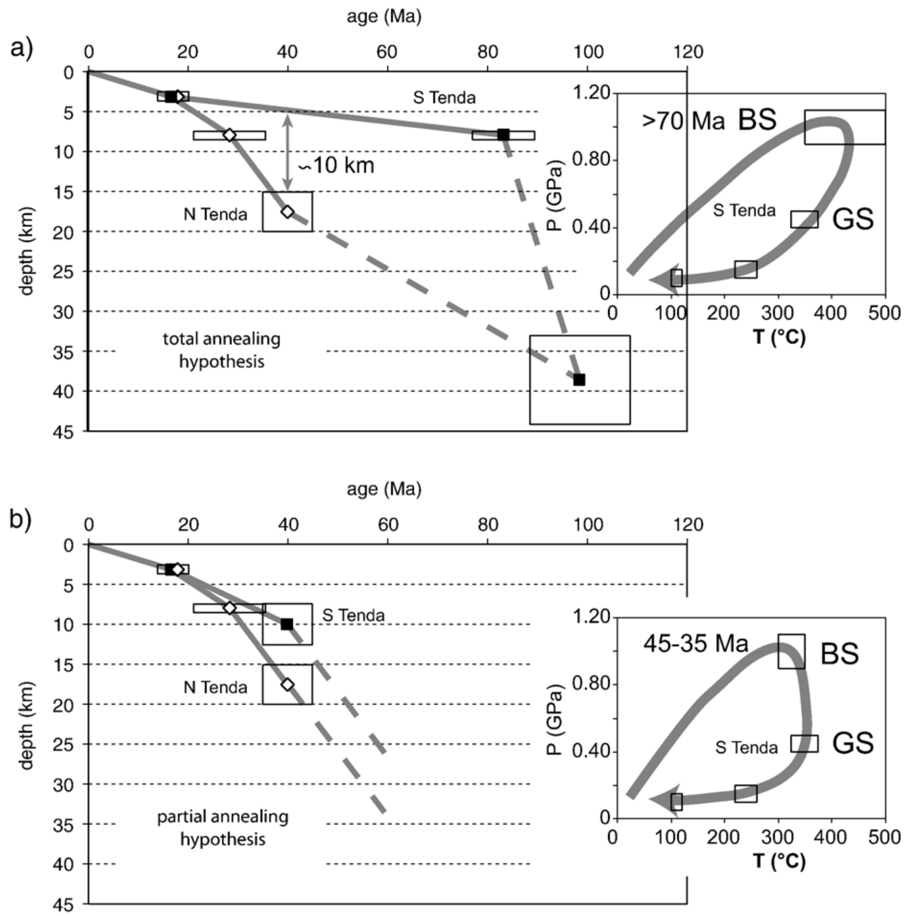

Fig. 8. Possible exhumation paths for the southern and northern parts of the Tenda massif: a) exhumation path derived assuming total annealing of the zircon fission-track ages in both the southern and northern Tenda massif; b) exhumation path derived assuming total annealing of zircon fission tracks in the northern Tenda massif and partial annealing of zircon fission tracks in the southern Tenda massif.

grains was necessary to obtain a good etch of the Hercynian Corsica samples, and these samples include only few countable low-U zircons that give the oldest ZFT ages in Corsica (Fig. 6). In contrast to the Hercynian basement samples, the Alpine Corsica samples showed a good etching behavior and easy countability, and the dated grains are distributed over a wide range of U content. The etching behavior and the FT ages of zircons from the metamorphosed granitoids shows that the temperature during the Alpine event was high enough to reset or partially reset the FT and also to heal the previous accumulated α-radiation damage. The second point illustrated by Fig. 6 is that U content varies significantly among the dated zircons (between 200 and 1100 ppm), although, the grains have similar source rocks (i.e. the Hercynian granitoids). Differing U-content results into uneven degree of radiation damage and produces a highly variable retentivity of zircons. Thus, the observed low χ^2 values could be explained in terms of different resistance of zircons to annealing implying variable annealing kinetics. In order to examine heterogeneous annealing of the ZFT samples and its significance in terms of thermal evolution, we have used the binomial peak-fitting method to analyze the zircon grain-age distribution (Brandon, 1996).

3.4. Zircon fission-track results and discussion

In the following sections we discuss our ZFT data in the light of geologic constraints and additional chronological data (apatite FT and ^{40}Ar–^{39}Ar data). In the first section we consider the ZFT data from southern and western Corsica, and the Corte region. In the second section we focus on the ZFT data from the Tenda massif and the Bastia area.

3.4.1. Hercynian basement and Corte region

Four samples from western Corsica (Hercynian basement) have ZFT ages between 161 and 114 Ma. Two of the sample localities are along the western Corsican coast, one is along the southeastern side of the island and one is in the core of the most elevated area of Corsica (Fig. 4). Analysis of the grain-age distribution provides insights into the thermal record of the samples. Grain ages of the four samples have been combined to a binomial peak-fitting statistical analysis, and in this way each zircon crystal is treated as a single observation. The grain-age distributions range between 242 and 76 Ma, and 56% of the grains belong to a 134 Ma population, while the younger ages cluster around 92 Ma, and the older ages cluster around 185 Ma (Fig. 7a). ZFT cooling ages in the range of 220–110 Ma are typical in the pre-Alpine basement of both European and African (Adria) continental margins (Vance, 1999; Bertotti et al., 1999). These ages can be related to high heat flow produced by mantle upwelling during Late Triassic and Jurassic continental rifting and subsequent drifting of the Ligure–Piemonte ocean basin, an arm of the Alpine Tethys. Thus, the ZFT grain ages in the Corsican Hercynian basement showing a peak at 134 Ma with a tail of older ages around 185 Ma can be interpreted as reflecting progressive cooling during the Alpine Tethys rifting and drifting.

Two samples from the Hercynian basement near the Alpine contact in the Corte region have ZFT ages of 87.5 and 70.9 Ma and both ages pass χ^2 (Fig. 4, Table 1). A sample from the same region but from a different unit, i.e. the Corte nappe stack bearing granites and granodiorites, has a ZFT age of 112.4 Ma and passes χ^2 (Fig. 4, Table 1). The grain-age distribution of the combined samples ranges between 57 and 144 Ma with 50% grains clustering around 77 Ma and 50% grains around 113 Ma (Fig. 7b). The Hercynian basement in this region and the granitoid rocks of the Corte units show a similar metamorphic overprint. The Hercynian

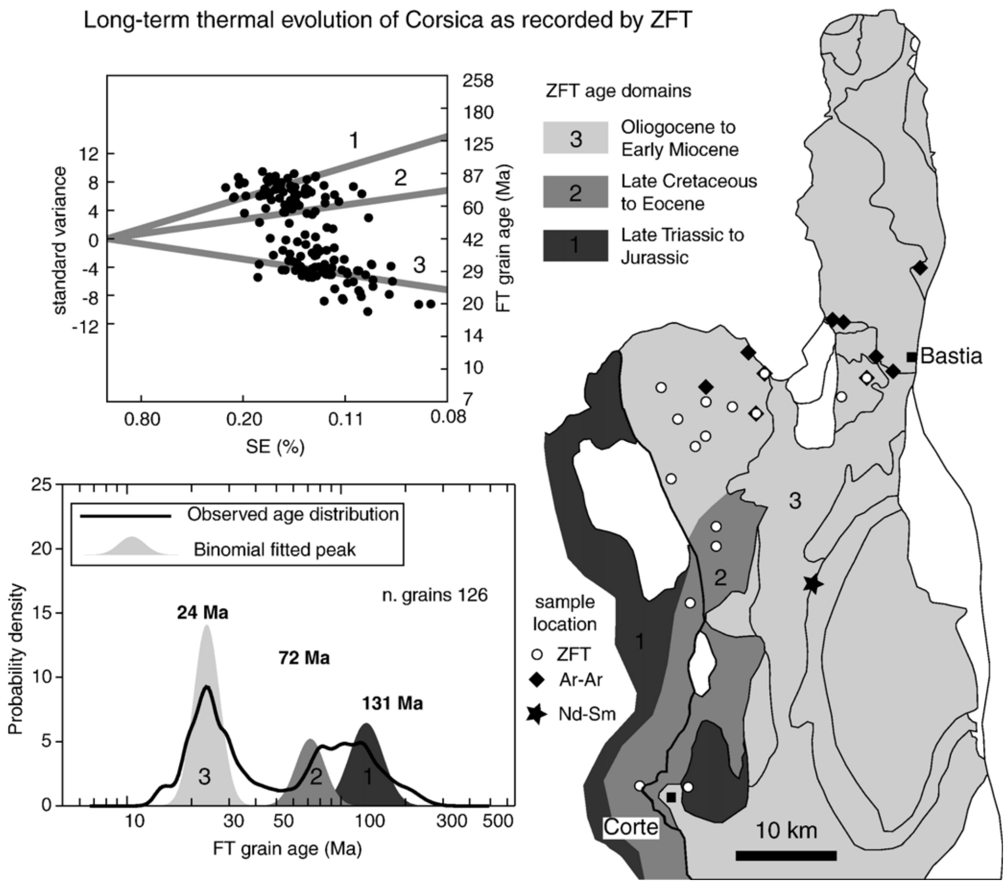

Fig. 9. Results of binomial peak-fitting (Brandon, 1996) for all zircon fission-track grain ages analyzed by this study. Results are represented through the radial (top) and probability density plots (bottom). On these plots, the observed distribution is reported together with the individual peaks representing the grain-age components. On the radial plots, zircon fission-track (ZFT) grain ages are represented by dots and the individual peaks by the gray lines. These plots show the long-term thermal evolution of Corsica as recorded by zircon fission tracks. These data indicate that Corsica records three main heating/cooling events during Late Triassic to Early Cretaceous, Late Cretaceous to Eocene and Oligocene to Early Miocene. The simplified map of northeastern Corsica represents the areas that record the three thermal events.

basement is strongly deformed and the sheared granitoids have mineral assemblages that reflect intermediate metamorphic conditions (Rossi et al., 1994) although peak pressure and temperature conditions have not been established. ^{40}Ar–^{39}Ar dating on K-feldspars from these granitoids gives an age of 35–40 Ma, which is inferred to represent the time of deformation (Maluski, 1977a,b). The sampled units of the Corte nappe stack unit were strongly affected by Alpine mylonitic to cataclastic deformation, and they have pumpellyite–prehnite mineral assemblages indicating lower greenschist metamorphic conditions (Amaudric du Chaffaut and Saliot, 1979; Rossi et al., 1994). Metamorphic conditions for the Corte nappe stack reached blueschist facies with peak temperatures ≤ 300 °C (Lahondère, 1991). In conclusion, the younger ZFT ages of ~77 Ma reflect a low-temperature Alpine overprint that only partially reset the zircons, whereas the old ages around 113 Ma are likely high-retentive zircons that fall in the range typical of zircons affected by Tethyan heating. Thus, during the Alpine event the temperature or the heating rate of these units did not reset completely the ZFT system.

3.4.2. Tenda massif and Oletta–Serra di Pigno units

Samples from orthogneiss of the northern Tenda massif and of the Oletta–Serra di Pigno units have ZFT ages that range from 36 to 19 Ma, but six out of ten samples fail χ^2 (Fig. 4, Table 1). The combined grain-age distribution of all single-grain ages ranges between 50 and 14 Ma (Fig. 7d). More than half of the grains (60%) belong to a peak age of ca. 25 Ma and lesser percentages correspond to peak ages of 40 and 18 Ma. The central ages of these samples are internally consistent and are younger than ^{40}Ar–^{39}Ar data that show plateau ages between 39 and 25 Ma (Brunet et al., 2000). Apatite FT ages from the same set of samples vary between 20 and 15 Ma, and thus both apatite and zircon FT ages clearly indicate a major cooling event at ca. 20 Ma as shown also by U–Th/He data on apatite (Zarki-Jakni et al., 2004; Fellin et al., 2005a,b). This event has been interpreted as related to rapid exhumation during Liguro–Provençal rifting and subsequent drifting. Grain-ages that cluster around 40 Ma may be partially annealed high-retentive zircons, and/or may record the onset of cooling after the Alpine metamorphism. This latter case would point to a progressive cooling event that started ~50 Ma.

Two samples from the southern Tenda massif have ZFT ages of 87.5 and 78.7 Ma and one fails χ^2 (Fig. 4, Table 1). The combined grain-age distribution for these two samples ranges from 105 to 56 Ma and two discrete grain-age populations can be identified at ~91 Ma and 66 Ma (Fig. 7c). No ^{40}Ar–^{39}Ar ages are available for this region, and AFT ages ranging between 20 and 14 Ma, so they do not usefully constrain the ZFT ages. In the Tenda massif, peak pressure and temperature during blueschist metamorphism is estimated at 0.8–1.0 GPa and 300–500 °C (Tribuzio and Giacomini, 2002). As reported by Brix et al. (2002), the high-pressure, low-temperature metamorphic rocks of Crete were affected by peak temperatures of 300 ± 50 °C for a heating duration of 4 ± 2 Ma and all these rocks have partially annealed ZFT ages regardless of the χ^2 test. Similarly, the Late Cretaceous ZFT ages in the southern Tenda massif could be partially annealed. If this is the case, during the Alpine event the southern Tenda massif experienced slightly lower temperature conditions than the northern Tenda. Another possible option is that the southern Tenda was buried for a shorter period of time than the northern Tenda, so that the heating duration was not enough to fully reset zircons. However, given the available constraints on the peak burial temperature for the Tenda massif, the hypothesis of completely reset ZFT ages in the southern part of the massif cannot be unequivocally discarded. This alternative explanation implies that the HP metamorphism in the Tenda massif is Late Cretaceous (Fig. 8), and also that the two sectors of the Tenda massif have significantly different exhumation histories. In fact, given an ^{40}Ar–^{39}Ar closure temperature of ~350–430 °C (e.g. Wijbrans and McDougall, 1986), and a ZFT closure temperature of ~240 °C, it follows that during the Eocene, the temperature difference between the northern and southern Tenda massif was significantly greater than 100 °C. Alternatively, assuming a rock density range of 2.5–2.7 g m^{-3}, uniform with depth, and deriving the burial depth from geobarometric data, during the Eocene the northern Tenda massif was buried at least at 15–20 km while the southern Tenda massif was at a depth shallower than 7–9 km, corresponding to the closure depth for the ZFT system for an exhumation rate of 1 km/Myr and a geothermal gradient of 20–30 °C/km (Fig. 8). Hence, totally reset Late Cretaceous ZFT ages in the southern Tenda massif imply a depth difference between the northern and southern Tenda massif of 6–13 km. At present, the distance between the Late Cretaceous samples in the southern sector and the Late Eocene to Early Miocene samples is ca. 10 km. Thus, restoration from the present relative position of the northern and southern Tenda to a past relative position of these two sectors with a depth difference of 6-to-13 km requires that a large differential exhumation has been accommodated over a short distance. Alternatively, a fault zone with major vertical displacement should separate the southern from the northern sector of the Tenda massif but major shear zones splitting the massif have not been recognized. Other alternative explanations should consider different thermal conditions during burial and subsequent exhumation of the two sectors of the massif. Variable thermal gradients and transient heat transfer effects have influenced the Neogene evolution of Corsica that at present displays over a length of ~180 km a significant horizontal gradient of surface heat flux with values between ~60 and 90 mW m^{-2} in the southern and northern regions, respectively (Pasquale et al., 1996). This heat flux pattern in Corsica clearly indicates significant lateral variations of the geothermal gradient, and these variations are interpreted as related to the formation of the Liguro–Provençal basin accompanied by magmatism during Oligocene to Early Miocene. Thus, at least since this time interval, the thermal regime has been far from equilibrium for most tectonic units in Alpine Corsica. In conclusion, as discussed also by previous studies (Mailhé et al., 1986) the different thermal record of the two sectors of the Tenda massif could be largely the result of different thermal conditions both during the Alpine metamorphism and the Oligocene–Miocene tectonic event.

3. Conclusions

ZFT ages record the long-term thermal evolution of Corsica. This thermal record is displayed in Fig. 9 where grain ages from all samples are plotted together both on a radial plot and on a probability density plot. These plots reveal three thermal overprints.

1) ZFT ages in the Hercynian basement of Western Corsica are 161–114 Ma and pre-date the Alpine metamorphic overprint. As elsewhere in the pre-Alpine basement of both European and African (Adria) continental margins, ZFT ages in the range 220–110 Ma are likely related to high heat flow associated with mantle upwelling during Late Triassic and Early Cretaceous continental rifting and subsequent opening of the Ligure–Piemonte ocean basin (Tethyan event; Vance, 1999; Bertotti et al., 1999).
2) Late Cretaceous ZFT ages from the Corsican Hercynian basement adjacent to the Alpine contact and in the Alpine units record the Alpine thermal overprint. These ages could be the result of partial annealing conditions related either to low geothermal gradient and temperatures ≤ 300 °C during the Alpine metamorphism, and/or to very rapid burial and subsequent exhumation. Alternatively these ages could be actual cooling ages reflecting total annealing during the Alpine event, and implying a Late Cretaceous subduction event.
3) Middle/Late Eocene to Early Miocene ZFT ages in the northern Tenda massif and in the Oletta–Serra di Pigno Units, together with the ^{40}Ar–^{39}Ar ages on mica (Brunet et al., 2000), FT and U–Th/He data on apatite (Cavazza et al., 2001; Zarki-Jakni et al., 2004; Fellin et al., 2005a,b) indicate cooling of the Alpine units from temperatures above 300 °C to below 70 °C between ~40 and 15 Ma. During this long interval, rocks of northern Corsica recorded cooling after the Alpine metamorphism and after the Oligocene–Early Miocene thermal perturbation related to the Liguro–Provençal basin formation. This perturbation is responsible for large lateral variation of the present heat flux of Corsica (Lucazeau and Mailhé, 1986; Pasquale et al., 1996), and in the Tenda massif it produced heat advection via rock uplift and extensional exhumation (Jolivet et al., 1990) followed by high cooling rates at shallow crustal levels (Cavazza et al., 2001; Fellin et al., 2005b).

Partial annealing better explains the Corsican Late Cretaceous ZFT ages than total annealing. This inference is supported by the most recent dating both in Alpine Corsica and in the internal Western Alps, indicating mostly Tertiary ages for the HP event, with the only exception of the Sesia Lanzo Zone (e.g. Dal Piaz et al., 2001). In addition, most ZFT ages in the internal Western Alps are younger than 40 Ma, whereas older ZFT ages are largely restricted to the Hercynian basement of the Southern Alps and of the external domains, and occur only locally in the low-grade units of the internal domain (e.g. Bernet et al., 2001).

A way to determine whether the Late Cretaceous ZFT ages of Corsica are partially or fully annealed would be to measure FT lengths because partially annealed samples would show shortened track lengths with respect to fully annealed samples. Unfortunately, the measurement of FT lengths in zircons is in its infancy because track revelation in zircon is very sensitive to etching conditions and standardized procedures have not yet emerged.

This study highlights the complexities of the ZFT system in rocks that have experienced multiple low-temperature heating/cooling events. The wide scatter of grain ages in some samples is caused in part by variations in track retentivity related to radiation damage. The use of central ages or mean ages for those samples with low chi-squared values fails to recognize much of the internal age structure in a sample. The analysis of grain-age distributions to isolate component populations, which are commonly geologically meaningful, is clearly advantageous. Further studies are needed to quantify the full extent of radiation damage on annealing kinetics, but for now we can use these subtle variations in track retention to elucidate low-temperature events.

Acknowledgments

We are greatly indebted to Vincenzo Picotti for stimulating discussions on the structural evolution of the Tenda massif. Mark T. Brandon has provided helpful insight into issues associated with radiation in zircon. We also acknowledge very helpful constructive reviews by Stuart Thompson and Francis Lucazeau.

References

Agard, P., Monié, P., Jolivet, L., Goffé, B., 2002. Exhumation of the Schistes Lustrés complex: in situ laser probe 40Ar/39Ar constraints and implications for the western Alps. J. Metamorph. Geol. 20, 599–618.

Amaudric du Chaffaut, S., Saliot, P., 1979. La région de Corte: secteur clé pour la compréhension du métamorphisme alpin en Corse. Bull. Soc. Géol. Fr. 21 (2), 149–154.

Bernet, M., Garver, J.I., 2005. Fission-track analysis of detrital zircon. Rev. Mineral. Geochem. 58, 205–238.

Bernet, M., Zattin, M., Garver, J.I., Brandon, M.T., Vance, J.A., 2001. Steady-state exhumation of the European Alps. Geology 29, 35–38.

Bertotti, G., Seward, D., Wijbrans, J., ter Voorde, M., Hurford, A.J., 1999. Crustal thermal regime prior to, during, and after rifting: a geochronological and modeling study of the Mesozoic south Alpine rifted margin. Tectonics 18, 185–200.

Bézert, P., Caby, R., 1988. Sur l'âge post-bartonien des événements tectono-métamorphiques alpin en bordure orientale de la Corse cristaline (Nord de Corte). Bull. Soc. Géol. Fr. 6, 965–971.

Boccaletti, M., Elter, P., Guazzone, G., 1971. Plate tectonics model for the developments of the western Alps and northern Apennines. Nature 234, 108–111.

Brandon, M.T., 1996. Probability density plot for fission-track grain-age samples. Radiat. Meas. 26, 663–676.

Brandon, M.T., Roden-Tice, M.K., Garver, J.I., 1998. Late Cenozoic exhumation of the Cascadia accretionary wedge in the Olympic Mountains, northwest Washington State. GSA Bull. 110 (8), 985–1009.

Brix, M.R., Stöckhert, B., Seidel, E., Theye, T., Thomson, S.N., Küster, M., 2002. Thermobarometric data from a fossil zircon partial annealing zone in high pressure-low temperature rocks of eastern and central Crete, Greece. Tectonophysics 349, 309–326.

Brunet, C., Monié, P., Jolivet, L., Cadet, J.-P., 2000. Migration of compression and extension in the Tyrrhenian Sea from $^{40}Ar/^{39}Ar$ ages on micas along a transect from Corsica to Tuscany. Tectonophysics 321, 127–155.

Cavazza, W., Zattin, M., Ventura, B., Zuffa, G.G., 2001. Apatite fission-track analysis of Neogene exhumation in northern Corsica (France). Terra Nova 13, 51–57.

Caron, J.M., 1994. Metamorphism and deformation in Alpine Corsica, Schweiz. Mineral. Petrogr. Mitt. 74, 105–114.

Caron, J.M., Pequignot, G., 1986. The transition between blueschists and lawsonite-bearing eclogites based on observations from Corsican metabasalts. Lithos 19, 205–218.

Cohen, C.R., Schweikert, R.A., Odom, A.L., 1981. Age of emplacement of the Schistes Lustrés Nappe, Alpine Corsica. Tectonophysics 72, 267–284.

Conchon, O., 1977. Néotectonique en Corse orientale d'après l'étude des formations quaternaires: comparaison entre la Marana et la plaine d'Aleria. Bull. Soc. Géol. Fr. 19 (3), 631–639.

Cubells, J.F., Ferrandini, J., Ferrandini, M., Gaudant, J., Loÿe-Pilot, M. D., 1994. Présence du genre Aphanius NARDO, famille des Cyprinodontidae, dans le Miocéne du Bassin de Francardo Ponte Leccia (Corse). Géol. Méditerr. 21 (1–2), 19–24.

Daniel, J.M., Jolivet, L., Goffe', B., Poinssot, C., 1996. Crustal-scale strain partitioning: footwall deformation below the Alpine Oligo-Miocene detachment of Corsica. J. Struct. Geol. 18 (1), 41–59.

Dal Piaz, G.V., Beccaluva, L., Bortolotti, V., Chiesa, S., Cimmino, F., Cortesogno, L., Ferrario, A., Lucchetti, G., Messiga, B., Spadea, P., Venturelli, G., Zanzucchi, G., Zirpoli, G., 1977. I complessi ofiolitici e le unità cristalline della Corsica alpina. Ofioliti 2 (2–3), 265–324.

Dal Piaz, G.V., Cortiana, G., Del Moro, A., Martin, S., Pennacchioni, G., Tartarotti, P., 2001. Tertiary age and paleostructural inferences of the eclogitic imprint in the Austroalpine outliers and Zermatt–Saas ophiolite, western Alps. Int. J. Earth Sci. 90, 668–684.

Dallan, L., Puccinelli, A., 1986. Geologia della regione del Nebbio (Corsica settentrionale). Bull. Soc. Geol. It. 105, 405–414.

Durand-Delga, M., 1984. Principaux traits de la Corse Alpine et corrélation avec les Alpes ligures. Mem. Soc. Geol. It. 28, 285–329.

Fellin, M.G., Picotti, V., Zattin, M., 2005a. Neogene to Quaternary rifting and inversion in Corsica: retreat and collision in the western Mediterranean. Tectonics 24, TC1011. doi:10.1029/2003TC001613.

Fellin, M.G., Zattin, M., Picotti, V., Reiners, P.W., Nicolescu, S., 2005b. Relief evolution in northern Corsica (western Mediterranean): constraints on uplift and erosion on long-term and short-term timescales. J. Geophys. Res. 110, F01016. doi:10.1029/2004JF000167.

Ferrandini, M., Ferrandini, J., Loÿe-Pilot, M.D., Butterlin, J., Cravette, J., Janin, M.C., 1998. Le Miocène du Bassin de Saint-Florent (Corse): Modalités de la transgression du Burdigalien Supérieur et mise en evidence du Serravallien. Geobios 31 (1), 125–137.

Galbraith, R.F., 1981. On statistical models for fission-track counts. J. Math. Geol. 13, 471–478.

Garver, J.I., Kamp, P.J.J., 2002. Integration of zircon color and zircon fission track zonation patterns in orogenic belts: application of the Southern Alps, New Zealand. Tectonophysics 349, 203–219.

Garver, J.I., Reiners, P.W., Walker, L.J., Ramage, J.M., Perry, S.E., 2005. Implications for timing of Andean uplift from thermal resetting of radiation-damaged zircon in the Cordillera Huayhuash, northern Peru. J. Geol. 113, 117–138.

Gattacceca, J., Orsini, J.-B., Bellot, J.-P., Henry, B., Rochette, P., Rossi, P., Cherchi, G., 2004. Magnetic fabric of granitoids from southern Corsica and northern Sardinia and implications for Late Hercynian tectonic setting. J. Geol. Soc. London 161, 277–289.

Gibbons, W., Horak, J., 1984. Alpine metamorphism of Hercynian hornblende granodiorite beneath the blueschists facies Schistes Lustrés nappe of NE Corsica. J. Metamorph. Geol. 2, 95–113.

Hurford, A.J., 1986. Cooling and uplift patterns in the Lepontine Alps, south central Switzerland, and an age of vertical movement on the Insubric fault line. Contrib. Mineral. Petrol. 92, 413–427.

Hurford, A.J., 1990. International union of geological sciences subcommission on geochronology recommendation for the standardization of fission track dating calibration and data reporting. Nucl. Tracks Radiat. Meas. 17, 233–236.

Jolivet, L., Dubois, R., Fournier, M., Goffé, B., Michard, A., Jourdan, C., 1990. Ductile extension in Alpine Corsica. Geology 18, 1007–1010.

Jolivet, L., Daniel, J.M., Fournier, M., 1991. Geometry and kinematics of ductile extension in Alpine Corsica. Earth Planet. Sci. Lett. 104, 278–291.

Jolivet, L., Faccenna, C., Goffè, B., Mattei, M., Rossetti, F., Brunet, C., Storti, F., Funiciello, R., Cadet, J.P., D'Agostino, N., Parra, T., 1998. Midcrustal shear zones in postorogenic extension: example from the northern Tyrrhenian Sea. J. Geophys. Res. 3 (B6), 12123–12160.

Lahondère, D., 1991. Les schistes bleus et les éclogites à lawsonite des unités continentales et océaniques de la Corse alpine: Nouvelles données pétrologiques et structurales. Thèse de 3ème cycle, Université Montpellier II, France.

Lahondère, D., Guerrot, C., 1997. Datation Nd–Sm du métamorphisme éclogitique en Corse alpine: un argument pour l'existence au Crétacé supérieur, d'une zone de subduction active localisée le long du bloc corso-sarde. Géol. Fr. 3, 3–11.

Lahondère, D., Rossi, Ph., Lahondère, J.C., 1999. Structuration Alpine d'une marge continentale externe: le massif du Tenda (Haute-Corse). Implications géodynamiques au niveau de la transversale Corse-Apennins. Géol. Fr. 4, 27–44.

Locke, B.D., Garver, J.I., 2005. Thermal evolution of the eastern Serranía del Interior foreland fold and thrust belt, northeastern Venezuela, based on apatite fission-track analyses. In: Avé Lallement, H.G., Sisson, V.B. (Eds.), Caribbean–South American Plate Interactions, Venezuela. Geological Society of America Special Paper, vol. 394, pp. 315–328.

Lucazeau, F., Mailhé, D., 1986. Heat flow, heat production and fission track data from the Hercynian basement around the Provençal Basin (western Mediterranean). Tectonophysics 128, 335–356.

Mailhé, D., Lucazeau, F., Vasseur, G., 1986. Uplift history of thrust belts: an approach based on fission track data and thermal modelization. Tectonophysics 124, 177–191.

Maluski, H., 1977a. Application de la methode ^{40}Ar–^{39}Ar aux mineraux des roches cristallines perturbees par des événements thermiques et tectoniques en Corse. Ph.D. Thesis, Université des Sciences et Techniques du Languedoc, Académie de Montpellier, France.

Maluski, H., 1977b. Application de la me´thode 40Ar/39Ar aux minéraux des roches cristallines perturbées par les événements thermiques et tectoniques en Corse. Bull. Soc. Géol. Fr. 19 (4), 849–855.

Maluski, H., Mattauer, M., Matte, P., 1973. Sur la présence de décrochements alpins en Corse. C. R. Acad. Sci, Paris 276, 703–712.

Malavieille, J., Chemenda, A.I., Larroque, C., 1998. Evolutionary model for Alpine Corsica: mechanism for ophiolite emplacement and exhumation of high-pressure rocks. Terra Nova 10 (6), 317–322.

Mattauer, M., Proust, F., 1976. La Corse alpine: un modèle de genèse du métamorphisme haute pression par subduction de croute continentale sous du matériel oceanique. C. R. Acad. Sci., Paris 282, 1249–1252.

Mattauer, M., Faure, M., Malavieille, J., 1981. Transverse lineation and large-scale structures related to Alpine obduction in Corsica. J. Struct. Geol. 3, 401–409.

Mauffret, A., Contrucci, I., 1999. Crustal structure of the northern Tyrrhenian Sea. In: Durand, B., Jolivet, L., Horváth, F., Séranne, M. (Eds.), The Mediterranean Basins: Tertiary Extension within the Alpine Orogen. Geol. Soc. London Spec. Publ., vol. 156, pp. 169–193.

Molli, G., Tribuzio, R., 2004. Shear zones and metamorphic signature of subducted continental crust as tracers of the evolution of the Corsica/Northern Apennine orogenic system. In: Alsop, G.I., Holdsworth, R.E., McCaffrey, K.J.W., Hand, M. (Eds.), Flow processes in faults and shear zones. Geol. Soc. London Spec. Publ., vol. 224, pp. 321–335.

Naeser, C.W., 1976. Fission-track dating. U.S. Geological Survey, Open File Report 76–190. 65 p.

Nardi, R., Puccinelli, A., Verani, M., 1978. Carta geologica della Balagne "sedimentaria" (Corsica) alla scala 1:25.000 e note illustrative. Boll. Soc. Geol. Ital. 97, 11–30.

Orszag-Sperber, F., Pilot, M.D., 1976. Grand traits du Néogene de Corse. Bull. Soc. Géol. Fr. 18, 1183–1187.

Ottaviani-Spella, M.-M., Girard, M., Cheilletz, A., 1996. Les ignimbrites burdigaliennes du Sud de la Corse. Petrologie et datation K–Ar. C. R. Acad. Sci. Paris 323 (II a), 771–778.

Padoa, E., Saccani, E., Durand-Delga, M., 2002. The Rio Magno Unit (Alpine Corsica): a review of its structural, stratigraphical and geochemical features and their geodynamic implications. Ofioliti 27 (1), 31–42.

Pasquale, V., Verdoya, M., Chiozzi, P., 1996. Heat flux and timing of the drifting stage in the Ligurian–Provençal basin (NW-Mediterranean). J. Geodyn. 21 (3), 205–222.

Peybernès, B., Durand-Delga, M., Cugny, P., 2001. Reconstitution, en Corse, au Jurassique moyen-supérieur, de la marge Européenne de l'océan Liguro-Piémontais, grâce à des niveaux repères à Praekurnubia crusei (foraminifère). C. R. Acad. Sci. Paris 332, 499–506.

Principi, G., Treves, B., 1984. Il sistema corso-appenninico come prisma d'accrezione. Riflessi sul poblema generale del limite Alpi-Apennini. Mem. Soc. Geol. Ital. 28, 549–576.

Rahn, M.K., Brandon, M.T., Batt, G.E., Garver, J.I., 2004. A zero model for fission-track annealing in zircon. Am. Mineral. 89, 473–484.

Rollet, N., Déverchère, J., Beslier, M.O., Guennoc, P., Réhault, J.P., Sosson, M., Turffert, C., 2002. Back arc extension, tectonic inheritance, and volcanism in the Ligurian Sea, Western Mediterranean. Tectonics 21 (3), 1–23.

Rossi, P., Cocherie, A., 1991. Genesis of a Variscan batholith: field, mineralogical and geochemical evidence from the Corsica–Sardinia batholith. Tectonophysics, The European Geotraverse, Part 7, vol. 195, pp. 319–346.

Rossi, P., Durand-Delga, M., Caron, J.M., Guieu, G., Conchon, O., Libourel, G., Loÿe-Pilot, M.D., 1994. Notice explicative de la Feuille Corte à 1/50 000, BRGM — Service géologique national, Orléans Cedex, France.

Rossi, P., Durand-Delga, M., Lahondère, J.-C., Lahondère, D., 2001. Notice explicative de la Feuille Santo-Pietro-di-Tenda à 1/50 000, BRGM — Service géologique national, Orléans Cedex, France.

Rubatto, D., Gebauer, D., Compagnoni, R., 1999. Dating of eclogite-facies zircons: the age of the Alpine metamorphism in the Sesia–Lanzo Zone (Western Alps). Earth Planet. Sci. Lett. 167, 141–158.

Saccani, E., Padoa, E., Tassinari, R., 2000. Preliminary data on the Pineto gabbroic massif and Nebbio basalts: progress toward the geochemical characterization of Alpine Corsica ophiolites. Ofioliti 25 (2), 75–85.

Stämpfli, G.M., Marchant, R.H., 1998. Geodynamic evolution of the Tethyan margins of the western Alps. In: Pfiffner, O.A., Lehner, P., Heitzman, P., Mueller, S., Steck, A. (Eds.), Deep Structure of the Swiss Alps. Result of NRP, vol. 20. Birkhaeuser Verlag, Basel, pp. 223–239.

Tagami, T., Shimada, C., 1996. Natural long-term annealing of the zircon fission track system around a granitic pluton. J. Geophys. Res. 101, 8245–8255.

Tagami, T., Carter, A., Hurford, A.J., 1996. Natural long-term annealing of the zircon fission-track system in Vienna Basin deep borehole samples: constraints upon the partial annealing zone and closure temperature. Chem. Geol. 130, 147–157.

Tagami, T., Galbraith, R.F., Yamada, R., Laslett, G.M., 1998. Revised annealing kinetics of fission tracks in zircon and geological implications. Adv. Fission-Track Geochronol. 99–112.

Treves, B., 1984. Orogenic belts as accretionary prisms: the example of the northern Apennines. Ofioliti 9, 577–618.

Tribuzio, R., Giacomini, F., 2002. Blueschist facies metamorphism of peralkaline rhyolites from the Tenda crystalline massif (northern Corsica): evidence for involvement in the Alpine subduction event? J. Metamorph. Geol. 20, 1–14.

Vance, J.A., 1999. Zircon fission track evidence for a Jurassic (Tethyan) thermal event in the western Alps. In: Martin, S., Polino, R. (Eds.), Proceedings of Fission Track Analysis: Theory and Applications. Mem. Sci. Geol., vol. 51/2, pp. 473–476.

Vigliotti, L., Langenheim, V.E., 1995. When did Sardinia stop rotating? New paleomagnetic results. Terra Res. 7, 424–435.

Warburton, J., 1986. The ophiolite-bearing Schistes Lustrés Nappe in Alpine Corsica: a model for the emplacement of ophiolites that have suffered HP/LT metamorphism. Geol. Soc. Am. Mem. 164, 313–331.

Waters, C.N., 1990. The Cenozoic tectonic evolution of Alpine Corsica. J. Geol. Soc. London 147, 811–824.

Wijbrans, J.R., McDougall, I., 1986. 40Ar/39Ar dating of white micas from an Alpine high-pressure metamorphic belt on Naxos (Greece): the resetting of the argon isotope system. Contrib. Mineral. Petrol. 93, 187–194.

Yamada, R., Tagami, T., Nishimura, S., Ito, H., 1995. Annealing kinetics of fission tracks in zircon: an experimental study. Chem. Geol. (Isot. Geosci. Sect.) 122, 249–258.

Zarki-Jakni, B., van der Beek, P., Poupeau, G., Sosson, M., Labrin, E., Rossi, P., Ferrandini, J., 2004. Cenozoic denudation of Corsica in response to Ligurian and Tyrrhenian extension: results from apatite fission track thermochronology. Tectonics 23, TC1003. doi:10.1029/2003TC001535.